Leukemia (2016) **30,** 873–882

www.nature.com/leu

ORIGINAL ARTICLE

FOXM1 is a therapeutic target for high-risk multiple myeloma

C Gu[1,2,8], Y Yang[1,3,8], R Sompallae[2,4], H Xu[3], VS Tompkins[2], C Holman[2], D Hose[5,6], H Goldschmidt[5,6], G Tricot[3,7], F Zhan[3,7,9] and S Janz[2,7,9]

The transcription factor forkhead box M1 (FOXM1) is a validated oncoprotein in solid cancers, but its role in malignant plasma cell tumors such as multiple myeloma (MM) is unknown. We analyzed publicly available MM data sets and found that overexpression of *FOXM1* prognosticates inferior outcome in a subset (~15%) of newly diagnosed cases, particularly patients with high-risk disease based on global gene expression changes. Follow-up studies using human myeloma cell lines (HMCLs) as the principal experimental model system demonstrated that enforced expression of FOXM1 increased growth, survival and clonogenicity of myeloma cells, whereas knockdown of FOXM1 abolished these features. In agreement with that, constitutive upregulation of FOXM1 promoted HMCL xenografts in laboratory mice, whereas inducible knockdown of FOXM1 led to growth inhibition. Expression of cyclin-dependent kinase 6 (CDK6) and NIMA-related kinase 2 (NEK2) was coregulated with FOXM1 in both HMCLs and myeloma patient samples, suggesting interaction of these three genes in a genetic network that may lend itself to targeting with small-drug inhibitors for new approaches to myeloma therapy and prevention. These results establish *FOXM1* as high-risk myeloma gene and provide support for the design and testing of FOXM1-targeted therapies specifically for the FOXM1^{High} subset of myeloma.

Leukemia (2016) **30,** 873–882; doi:10.1038/leu.2015.334

INTRODUCTION

The prognosis of patients with multiple myeloma (MM), a difficult-to-cure blood cancer, depends in large measure on the genetic makeup of the myeloma cell. This is reflected in risk stratification models that consider cytogenetic features of myeloma, such as occurrence of oncogene-activating chromosomal translocations, and molecular features, such as gene expression changes[1] measured with the assistance of the UAMS-70,[2] EMC-92[ref. 3] or REL-17[ref. 4] gene test, to assign newly diagnosed cases to either standard- or high-risk groups. The distinction is clinically relevant because patients with high-risk myeloma have poor outcomes. Whereas overall survival (OS) for patients with standard-risk myeloma is 6–7 years, that for high-risk disease is no more than 2–3 years—despite the application of aggressive, risk-adapted therapies that include new myeloma drugs and, for eligible patients, high-dose therapy followed by autologous stem cell transplantation.[5] The unmet medical need of high-risk myeloma calls for dedicated efforts to elucidate the underlying genetic networks and develop approaches for their therapeutic targeting. This study demonstrates the involvement of the transcription factor forkhead box M1 (FOXM1) in a significant subset of high-risk myeloma (~15%) and suggests that FOXM1 provides a molecularly targeted treatment opportunity specifically for this group of patients.

In 2010, based on its enormous potential for the diagnosis and therapy of solid cancers, the AAAS journal *Science* bestowed upon FOXM1 the 'Breakthrough of the Year' award. *FOXM1*, a member of the large forkhead box (FOX) family of proteins ($n \approx 50$), is a validated oncogene in carcinomas,[6] but has received little attention in myeloma and related plasma cell malignancies. Findings implicating FOXM1 in the maintenance and self-renewal of carcinoma stem cells[7] have raised the question of whether it is similarly important for the putative myeloma stem cell[8]—yet the elusiveness of this cell[9] stands in the way of resolving the issue. Consistent with results that the expression of FOXM1 is tightly regulated in normal cells to ensure mitotic fidelity throughout the cell cycle,[10] deregulated expression of FOXM1 in carcinoma cells leads to centrosome amplification, mitotic catastrophe and other cytogenetic aberrations typically seen in cancer cells.[11] Whether FOXM1 governs genomic instability of MM,[12] a notorious but ill-explained feature of the neoplasia, is unclear. In diffuse large B-cell lymphoma, in which levels of the *FOXM1* mRNA and the encoded protein are high, targeted inhibition of FOXM1 augments cell killing when combined with normally subtoxic doses of the proteasome inhibitor, bortezomib.[13] Whether this holds true for MM has not been established.

Our interest in FOXM1 began with a comparative gene expression analysis of B-lymphoma counterparts in humans and mice, implicating the transcription factor in an evolutionarily conserved pathway of neoplastic B-cell development.[14] Further encouraged by new evidence indicating that FOXM1 (1) drives tumor development and progression[15–19] by virtue of a complex mechanism that includes enhanced cell proliferation, migration and invasion,[6] regulation of the DNA damage response[20] and changes in the cancer epigenome,[21] (2) promotes cancer cell resistance to ionizing radiation[22] and cytotoxic drugs,[23]

[1]Basic Medical College, Nanjing University of Chinese Medicine, Nanjing, People's Republic of China; [2]Department of Pathology, The University of Iowa Roy J and Lucille A Carver College of Medicine, Iowa City, IA, USA; [3]Department of Internal Medicine, The University of Iowa Roy J and Lucille A Carver College of Medicine, Iowa City, IA, USA; [4]Iowa Institute of Human Genetics, University of Iowa, Iowa City, IA, USA; [5]Medizinische Klinik V, Universitätsklinikum Heidelberg, Heidelberg, Germany; [6]Nationales Centrum für Tumorerkrankungen, Heidelberg, Germany and [7]Holden Comprehensive Cancer Center, The University of Iowa Roy J and Lucille A Carver College of Medicine, Iowa City, IA, USA. Correspondence: Professor F Zhan, Department of Internal Medicine, The University of Iowa Roy J and Lucille A Carver College of Medicine, Iowa City, IA 52242, USA or Professor S Janz, Department of Pathology, The University of Iowa Roy J and Lucille A Carver College of Medicine, Iowa City, IA 52242, USA.
E-mail: fenghuang-zhan@uiowa.edu (FZ) or siegfried-janz@uiowa.edu (SJ)
[8]These author are co-first authors.
[9]These author are co-senior authors.
Received 28 August 2015; revised 5 November 2015; accepted 24 November 2015; accepted article preview online 9 December 2015; advance online publication, 26 January 2016

(3) governs, in part, the survival and tissue-regenerating capacity of both normal hematopoietic stem cells[24] and malignant stem cell-like cells,[25] (4) links acquired resistance to cancer therapy with cancer stemness[26] and (5) owing to the development of specific small-molecule inhibitors,[27] it may soon be targeted more effectively than possible in the past;[28] we here decided to evaluate whether FOXM1 might have an important but heretofore overlooked role in plasma cell myeloma.

MATERIALS AND METHODS

FOXM1 expression and survival analysis in patients with myeloma

Levels of *FOXM1* mRNA in myeloma cells were determined using Affymetrix U133Plus 2.0 microarrays (Affymetrix, Santa Clara, CA, USA) as described previously.[1] Results are available in the NIH Gene Expression Omnibus (GEO) under accession number GSE2658. Microarray data on monoclonal gammopathy of undetermined significance and normal plasma cells are available at GSE5900. Statistical analysis of microarray results relied on GCOS1.1 software (Affymetrix), including log-rank tests for univariate association with disease-related survival.

HMCLs, antibodies and reagents

Human myeloma cell line (HMCLs), designated H929 or APR1, were chosen for studies on inducible knockdown (KD) of FOXM1. HMCLs, CAG or XG1 were used for studies on constitutive overexpression (OE) of FOXM1. All four cell lines had secretion of IgA[29–32] and *in vitro* culture conditions (37 °C, 5% CO_2) in common. Oncogene-activating chromosomal translocations took the form of t(4;14) in case of H929 cells,[33] t(11;14) in XG1 cells[30] and t(14;16) in ARP1 and CAG cells.[33,34] Gene expression spikes on microarrays corresponded to the translocation status: *FGFR3* and *WHSC1* (better known as *MMSET*) in case of H929 cells, *CCND1* (cyclin D1) in XG1 cells and *MAF* (c-MAF) in ARP1 and CAG cells.[35] The status of the tumor suppressor p53 was wild type in case of H929 cells,[36] mutated in XG1 cells[37] and null in ARP1 and CAG cells.[34] Antibodies for western blotting were purchased from Santa Cruz Biotechnology (Dallas, TX, USA) (FOXM1, catalog number sc-500; CDK6 (cyclin-dependent kinase 6), sc-7961; β-actin, sc-47778) or Cell Signaling Technology (Danvers, MA, USA) (caspase-8, 4927; cleaved caspase-8, 9496; caspase-9, 9502; caspase-3, 9668; cleaved caspase-3, 9661; PARP, 9542). Dox and thiostrepton (TS) were from Sigma-Aldrich (St Louis, MO, USA).

Quantitative, reverse transcription polymerase chain reaction

Total RNA was extracted using Quick-RNA MiniPrep (Zymo Research, Irvine, CA, USA) and reverse transcribed using oligo dT primers and SuperScript III RT (Invitrogen, Carlsbad, CA, USA). Data analysis relied on the ΔΔCt method. Primers were purchased from Integrated DNA Technologies (Coralville, IA, USA). Sequences are available upon request.

Western blotting and co-immunoprecipitation assays

Whole myeloma cell lysates were prepared using the Mammalian Cell Extraction Kit (K269-500) from Biovision (Milpitas, CA, USA). Proteins (30 μg per sample) were fractionated on 4–12% polyacrylamide gels blocked with 5% non-fat milk in Tris-buffered saline containing 0.05% Tween-20. Proteins were transferred to nitrocellulose membranes, incubated with primary antibody (dilution 10^{-3}) overnight (4 °C) and visualized with horse radish peroxidase-conjugated secondary antibody using SuperSignal West Pico (Pierce Biotechnology, Rockford, IL, USA). Blots were stripped, reprobed for β-actin and evaluated by densitometry to estimate protein abundance. Co-immunoprecipitations (co-IPs) using the Pierce Direct Magnetic IP/Co-IP Kit (Thermo Scientific, Rockford, IL, USA) and antibodies to FOXM1 and CDK6 were performed as recently described.[38] IgG from Bethyl Laboratories (Montgomery, TX, USA) was used as control.

Soft-agar clonogenicity assay

Clonogenic growth of myeloma was evaluated by seeding 1×10^4 cells in 0.5 ml RPMI 1640 (Invitrogen) supplemented with 0.33% agar and 10% FBS. Cells were grown *in vitro* (37 °C, 5% CO_2) for 3 weeks, replenishing cell culture medium twice weekly. In some cases, cells were treated during weeks 2 and 3 with the FOXM1-inhibiting thiazole antibiotic, TS. Cell clones, defined as tight aggregates of ⩾40 myeloma cells, were enumerated using photographic images of soft-agar plates uploaded to Image J.

Cell proliferation and viability

Cell proliferation rate and viability were determined in 6-well plates using a hemacytometer and the trypan blue exclusion assay (0.4% dye in phosphate-buffered saline, pH 7.3).

Myeloma xenografts in immune-compromised laboratory mice

To evaluate the impact of FOXM1 KD on myeloma growth, 2×10^6 H929 cells expressing either normal ($FOXM1^N$) or reduced ($FOXM1^{KD}$) levels of FOXM1 were injected subcutaneously into the right and left flank,

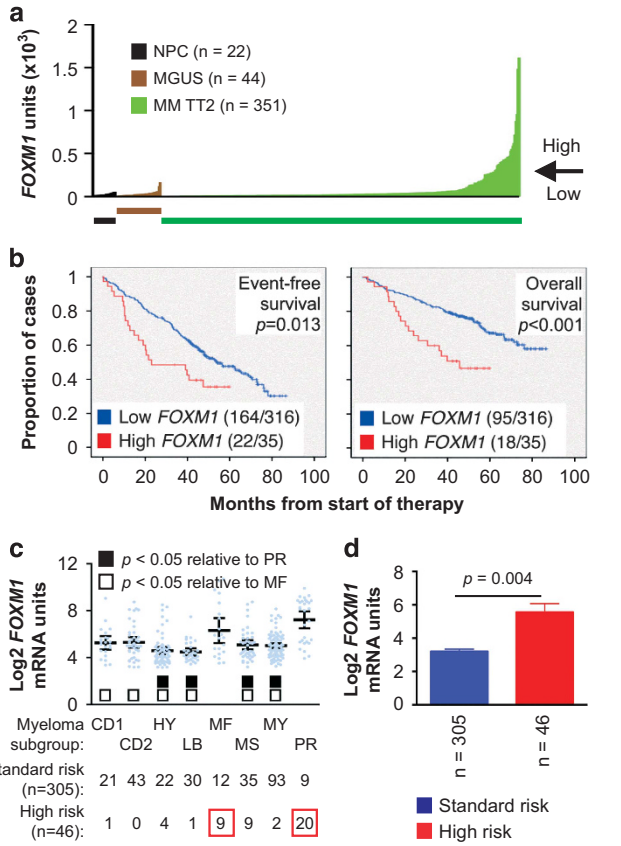

Figure 1. *FOXM1* mRNA levels predict poor survival in a subset of patients with newly diagnosed myeloma. (**a**) Line graph depicting the range of *FOXM1* mRNA levels (gene probe ID 202580) in normal BM plasma cells (NPC), 'premalignant' BM plasma cells from individuals with monoclonal gammopathy of undetermined significance (MGUS) or malignant plasma cells from patients with newly diagnosed MM from the University of Arkansas TT2 cohort. Specimens exhibiting < or >200 U of *FOXM1* message were categorized as $FOXM1^{Low}$ and $FOXM1^{High}$, respectively. This is indicated by the horizontal, labeled arrow pointing left. (**b**) Reduced EFS and OS in newly diagnosed TT2 patients harboring high *FOXM1* levels. Of 351 myeloma cases, 316 (90%) had low *FOXM1* levels (blue curve) and 35 (10%) had high *FOXM1* levels (red curve). EFS and OS data were available from 186 (53%) and 113 (32%) patients, respectively. (**c**) Mean values of *FOXM1* levels in eight molecular subgroups of MM: CD1, CCND1/CCND3 group 1; CD2, CCND1/CCND3 group 2; HY, hyperdiploid; LB, low bone disease; MF, MAF/MAFB; MS, MMSET; MY, myeloid; PR, proliferation.[2] *FOXM1* is significantly elevated in MF myelomas as compared with six subgroups with low *FOXM1* levels (open squares), and in the PR myelomas as compared to four such subgroups (closed squares), as assessed using the Bonferoni *t*-test. The number of patients within each molecular subgroup who exhibit the standard- or high-risk UAMS-70 gene signature is indicated at the bottom. In total, 46 of 351 patients fell into the high-risk category, with at least one case in each of the molecular subgroups except CD2. (**d**) *FOXM1* expression in high-risk MM, as defined by the UAMS-70 gene signature ($n = 46$), is elevated compared with that in low-risk MM ($n = 305$; Mann–Whitney test).

respectively, of NSG (NOD scid gamma) mice (Jackson Laboratory, Bar Harbor, ME, USA). To induce FOXM1 KD in incipient tumors, Dox (2 mg/ml) was added to the drinking water, beginning on day 10 following myeloma cell transfer.

Similarly, to assess the effect of FOXM1 OE on myeloma growth, paired samples of CAG cells (2 million in each flank) that expressed either elevated levels of FOXM1 ($FOXM1^{OE}$) or normal levels ($FOXM1^{N}$) were transferred subcutaneously to NSG mice (Jackson Laboratory). After 10 days, some mice were treated with intraperitoneal administrations of TS (30 mg/kg) twice weekly. In all cases, tumor growth was measured two to three times weekly, using a pair of calipers. Mice were killed using CO_2 asphyxiation when tumors reached 20 mm in diameter. All studies were approved under protocol 1301010 of the Institutional Animal Care and Use Committee of The University of Iowa.

Statistical analysis

Two-tailed Student's *t*-test was used to compare two experimental groups. One-way analysis of variance was used to evaluate more than two groups. The Kaplan–Meier method was used to determine myeloma patient survival in accordance with *FOXM1* expression. In all cases, $P \leqslant 0.05$ was considered significant.

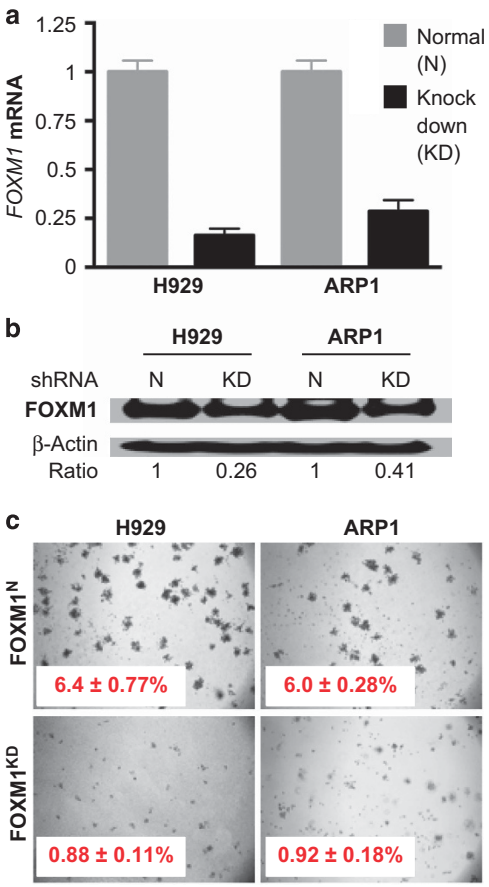

Figure 2. Genetic KD of FOXM1 mitigates clonogenicity of myeloma *in vitro*. (**a**) *FOXM1* message levels in H929 and ARP1 myeloma cells, using qRT-PCR as the measurement tool. Cells either under-expressed FOXM1 because of lentiviral transduction of a *FOXM1*-targeted shRNA 'KD' construct (KD) or expressed FOXM1 at normal levels (N) following transduction of a non-targeted or 'scrambled' shRNA used as the control. Average loss of *FOXM1* mRNA upon gene KD was ~80% and ~70% in H929 and ARP1 cells, respectively. (**b**) Western blot analysis of samples included in panel a. Whole-cell lysates were electrophoretically fractionated and immunoblotted using antibodies to FOXM1 and β-actin. Densitometry was used to determine the FOXM1-to-β-actin ratio. Loss of FOXM1 protein in H929 and ARP1 KD cells amounted to 74% and 59%, respectively. (**c**) Photographic images of representative soft-agar plates indicating the decreased clonogenic growth of $FOXM1^{KD}$ cells (bottom) compared with $FOXM1^{N}$ cells (top).

RESULTS

Heightened *FOXM1* expression predicts poor survival in patients with myeloma

To evaluate the possibility that FOXM1 is important for myeloma, we analyzed a well-annotated, mature data set, designated total therapy 2 (TT2), for which microarray-based gene expression and clinical outcome data were available. The levels of *FOXM1* in 351

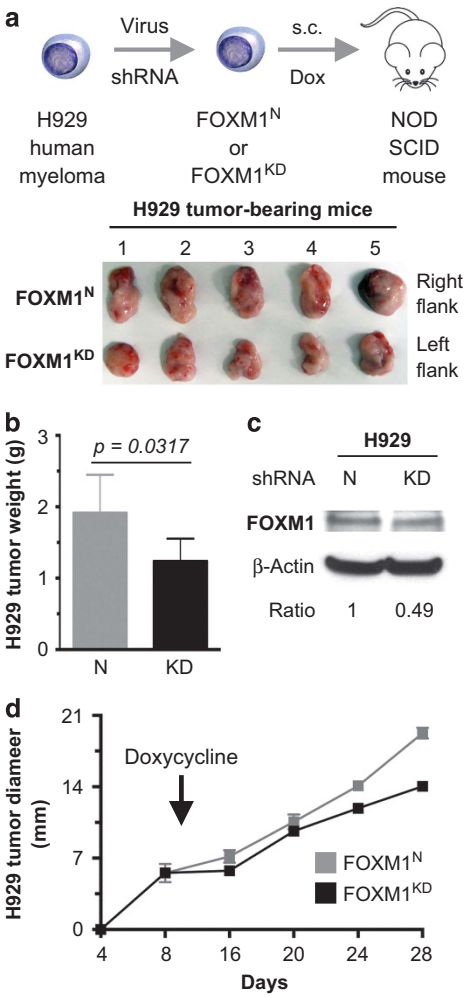

Figure 3. Inducible downregulation of FOXM1 inhibits myeloma xenografts in NSG mice. (**a**) Shown at the top is a scheme of the study design. $FOXM1^{KD}$ and $FOXM1^{N}$ H929 cells, generated using lentiviral shRNA transduction, were xenografted subcutaneously (s.c.) into the left and right flank of NSG hosts, respectively. After 10 days, mice received doxycycline in the drinking water to induce *FOXM1*-targeted shRNA in case of KD cells and scrambled shRNA in case of N cells. On day 28, xenografts were harvested and photographic images were taken (bottom). (**b**) Mean weight of $FOXM1^{KD}$ and $FOXM1^{N}$ xenografts on day-28 postmyeloma cell transfer. (**c**) Western blot analysis comparing FOXM1 protein levels in day-28 $FOXM1^{KD}$ and $FOXM1^{N}$ xenografts. (**d**) Time course of tumor growth in NSG mice. Doxycycline treatment of mice began 10 days after myeloma cell transfer, as indicated by a vertical, labeled arrow pointing down. Tumor diameters were measured using a caliper, beginning on day 8 after xenografting. Mice were killed on day 28. Mean tumor diameters (squares) and standard deviations of the mean (short vertical lines with error bars) are plotted. Regression analysis of growth rates demonstrated that the $FOXM1^{KD}$ tumors ($y = 0.665x + 0.0295$; $r^2 = 0.948$; $P < 10^{-3}$) lagged behind their $FOXM1^{N}$ counterparts ($y = 0.896x + 0.0280$; $r^2 = 0.973$; $P < 10^{-3}$) by ~25%. The area under the curve of the $FOXM1^{KD}$ tumors (160) was ~15% smaller than that of the $FOXM1^{N}$ (188) tumors.

patients with newly diagnosed myeloma from that data set are presented in Figure 1a, according to increasing gene expression. With 200 units of *FOXM1* message used as a cutoff, the great majority of cases (316/351, 90%) exhibited the same expression levels seen in normal plasma cells from the bone marrow (BM; $n=22$) or in BM plasma cells from individuals with monoclonal gammopathy of undetermined significance ($n=44$), a precursor of frank myeloma.[39] However, in 10% of myelomas (35/351) *FOXM1* levels were grossly elevated. The distinction between high and low *FOXM1* was of prognostic significance, as both event-free survival (EFS) and OS were reduced in cases exhibiting high *FOXM1* expression (Figure 1b). A very similar fraction of '*FOXM1*^{High}' myelomas (18/149, 12.1%; Supplementary Figure 1a) associated with the same kind of survival disadvantage (Supplementary Figure 1b) was seen in the Total Therapy 3 (TT3) cohort, which comprised intensively treated patients ($n=149$) who had received tandem autologous stem cell transplantation and bortezomib/thalidomide-based induction and maintenance.[40] Similarly, elevated *FOXM1* message predicted poor OS of patients with myeloma ($n=247$) treated upfront using high-dose therapy/autologous stem cell transplantation at the University of Heidelberg (Heidelberg, Germany) (Supplementary Figure 2).[41] In agreement with the variable *FOXM1* message levels seen in TT2/3 myelomas, a pilot immunolabeling study of archival myeloma-laden BM sections pointed to variable amounts and distribution patterns of FOXM1 protein in myeloma cells (Supplementary Figure 3). These findings indicated that upregulation of *FOXM1* in a subset of myeloma (10–12%) leads to inferior outcome.

FOXM1 is a high-risk myeloma gene

We asked whether heightened *FOXM1* expression in the TT2 cohort might be associated with a particular molecular subgroup of myeloma. Figure 1c presents the mean values of *FOXM1* levels in eight widely recognized subgroups, showing that elevated *FOXM1* was particularly prevalent in two known to confer high risk in terms of clinical course and outcome: MAF/MAFB (MF) and proliferation (PR). A more recently developed molecular genetic approach to distinguishing high- and standard-risk disease, that is, the UAMS-70 gene signature,[2] afforded another way of testing whether upregulated *FOXM1* might be a feature of high-risk myeloma. Statistical comparison of the mean *FOXM1* levels in the 46 and 305 cases identified as high and standard risk according to this signature supported this contention (Figure 1d). In sync with that, not only was FOXM1^{High} status statistically linked (χ^2 contingency analysis) with a positive score in the 70-gene test ($P<10^{-4}$) but almost two-thirds of the UAMS-70 high-risk cases (29/46, 63%) fell into the PR ($n=20$) and MF ($n=9$) subgroups of myeloma (indicated by red squares in Figure 1c, bottom). The TT3 myelomas exhibited the same preponderance of *FOXM1*^{High} in the MF/PR subgroups and the same association of *FOXM1*^{High} status and positive 70-gene test score seen in the TT2 sample (Supplementary Figures 1c and d). The findings in more than 500 myelomas from the TT2/3 studies led us to conclude that *FOXM1* is a *bona fide* high-risk myeloma gene.

Inducible downregulation of FOXM1 inhibits myeloma cells *in vitro*

Following up on the clinical observations described above, we decided to elucidate the role of FOXM1 in myeloma biology using two independent HMCLs, designated H929 and ARP1, that harbored ample amounts of FOXM1 protein. To evaluate whether short hairpin RNA (shRNA)-mediated KD of *FOXM1* message blunts the growth and survival of myeloma, we transduced H929 and ARP1 cells with lentivirus that encoded a *FOXM1*-targeted shRNA under the control of a Dox-inducible gene promoter: FOXM1^{KD} cells. Cells transduced with a Dox-inducible 'scrambled' shRNA, not targeting any expressed gene in mice and therefore leaving FOXM1 at normal levels (N), were used as control: FOXM1^{N} cells.

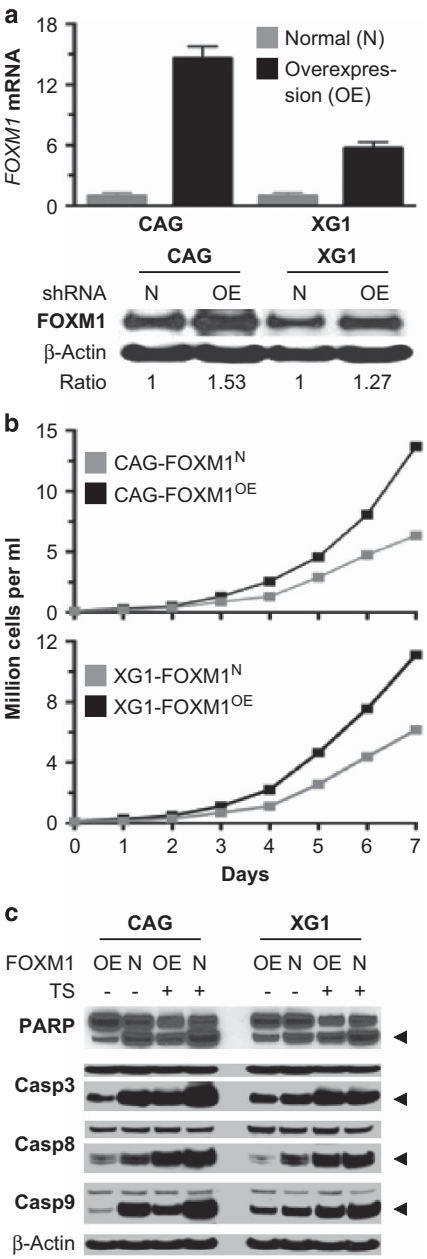

Figure 4. Enforced expression of FOXM1 promotes growth and survival of myeloma cells *in vitro*. (**a**) *FOXM1* message levels measured by qRT-PCR (top) and FOXM1 protein levels determined by western blotting (bottom) in CAG and XG1 myeloma cells that were either overexpressing FOXM1 constitutively because of lentiviral transduction of a *FOXM1* cDNA gene (OE) or containing normal amounts of FOXM1 (N) because of transduction of an 'empty' virus. The average increase in *FOXM1* mRNA in OE cells was ~14- and ~6-fold in CAG and XG1 cells, respectively. The corresponding increase in FOXM1 protein was more modest, as indicated by the FOXM1-to-actin ratio below the western blot analysis. (**b**) Line graphs depicting the growth of FOXM1^{OE} and FOXM1^{N} CAG (top) or XG1 (bottom) cells during 1 week in cell culture. OE cells grew faster than N cells, using two-way analysis of variance (ANOVA) for statistical comparison ($P<0.05$). (**c**) Western blot analysis of whole-cell lysates of FOXM1^{OE} and FOXM1^{N} CAG (left) and XG1 (right) cells, using as detection tools specific antibodies to poly (ADP-ribose) polymerase (PARP) or three members of the apoptosis-related cysteine peptidase family of caspase proteins. Myeloma cells were either treated (indicated by '+' sign) using the FOXM1 inhibitor TS or left untreated (indicated by '−' sign).

Quantitative, reverse transcription-PCR ((qRT-PCR) and western blot analyses demonstrated successful KD of FOXM1 in both cell lines at the mRNA (Figure 2a) and protein (Figure 2b) level. Significant reductions in $FOXM1^{KD}$ cell numbers, relative to $FOXM1^{N}$ controls, after 2, 3 and 4 days of Dox-dependent expression of shRNA indicated that partial loss of FOXM1 hampers myeloma growth *in vitro* (Supplementary Figure 4a). The diminished growth rate of $FOXM1^{KD}$ cells was attributed to both increased apoptotic cell death evidenced by increased proteolytic cleavage of poly (ADP-ribose) polymerase and caspases 3, 8 and 9 (Supplementary Figure 4b) and reduced cell cycle progression. The latter was revealed by flow cytometric analysis of DNA content that demonstrated an increase of cells in the G1 phase and a concomitant decrease in the S and G2/M phases (not shown). Soft-agar clonogenicity assays demonstrated a striking (~7-fold) drop in size and number of $FOXM1^{KD}$ versus $FOXM1^{N}$ colonies: 0.88% vs 6.4% in case of H929 cells and 0.92% vs 6.0% in case of ARP1 cells (Figure 2c). These results suggested that FOXM1 regulates, in part, the growth and survival of myeloma cells.

Genetic targeting of FOXM1 retards myeloma growth in mice

To determine whether inducible KD of *FOXM1* inhibits myeloma *in vivo*, we xenografted $FOXM1^{KD}$ and $FOXM1^{N}$ H929 cells under the skin of the left and right abdominal flank of NSG mice ($n = 5$), respectively. Ten days after *in vivo* transfer of two million cells to each side, the mice were administered Dox in the drinking water to induce the expression of FOXM1-targeted or scrambled shRNA in the malignant plasma cells (Figure 3a, top). Tumor diameters were measured daily, using a pair of calipers, to compare the growth rate of the paired $FOXM1^{KD}$ and $FOXM1^{N}$ xenografts. In five of five hosts, the $FOXM1^{KD}$ tumors harvested on day 28 (end point of study) were visibly smaller than their $FOXM1^{N}$ counterparts (Figure 3a, bottom). The mean weight of $FOXM1^{KD}$ tumors (1.24 g) was 35% lower compared with that of $FOXM1^{N}$ tumors (1.91 g; Figure 3b). Compared with $FOXM1^{N}$ tumors, $FOXM1^{KD}$ tumors contained reduced amounts of FOXM1 protein (Figure 3c). Comparison of growth rates demonstrated that the $FOXM1^{KD}$ tumors lagged behind their $FOXM1^{N}$ counterparts (Figure 3d), indicating stable expression of the FOXM1-targeted

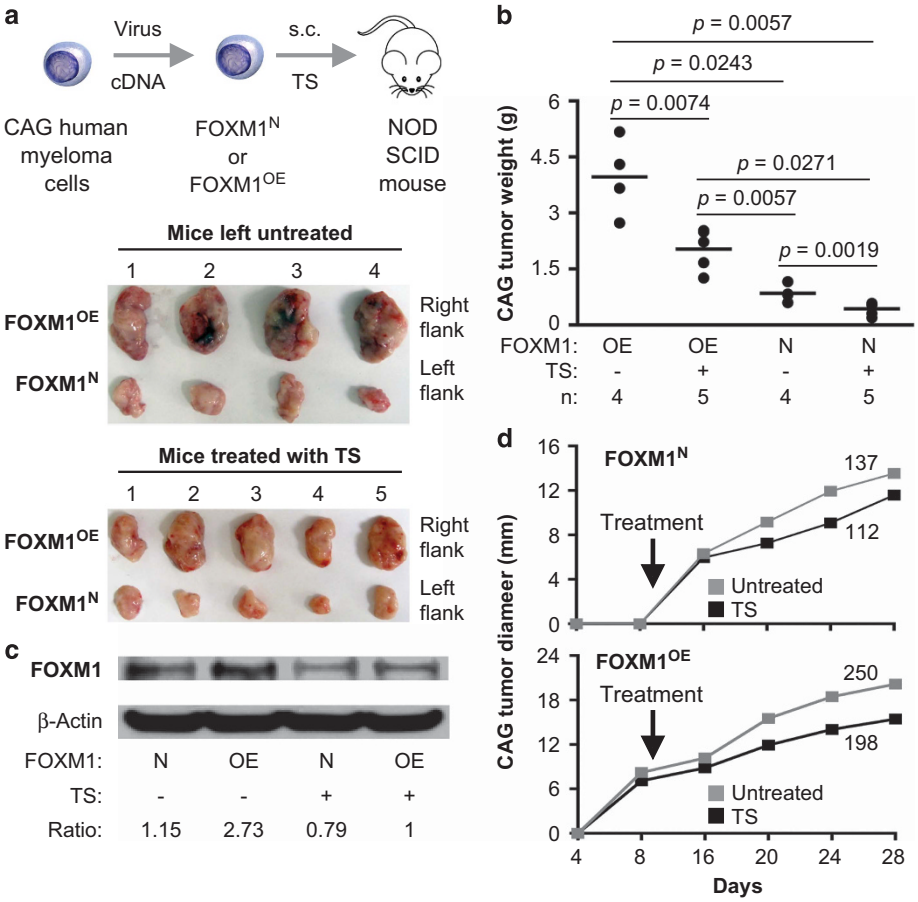

Figure 5. Treatment of NSG mice with TS inhibits $FOXM1^{OE}$ xenografts more effectively than $FOXM1^{N}$ xenografts. (**a**) Scheme of experimental approach (top) and photographic images of myeloma xenografts harvested upon study termination on day 28 (bottom). $FOXM1^{OE}$ and $FOXM1^{N}$ CAG cells were generated using *in vitro* lentiviral gene transduction, followed by xenografting subcutaneously into the right and left flank of NSG hosts, respectively. One half of the study group was treated with TS (30 mg/kg intraperitoneally twice weekly) beginning on day 10 after cell transfer, whereas the other half was left untreated. (**b**) Mean tumor weights (indicated by horizontal lines) in the four experimental groups at the end of study on day 28 after cell transfer. Tumor weights in TS-treated mice were smaller than that in untreated mice (*P*-values of Mann–Whitney tests are indicated) in case of both $FOXM1^{OE}$ and $FOXM1^{N}$ xenografts. The magnitude of TS-dependent tumor reduction was ~8 times higher in OE samples (4.2–2.6 g = 1.6 g) compared with N samples (0.8–0.6 g = 0.2 g). (**c**) Representative western blot analysis of FOXM1 protein levels in $FOXM1^{OE}$ and $FOXM1^{N}$ xenografts collected from TS-treated ('+') or untreated ('−') hosts on day 28 after cell transfer. The ratios of FOXM1 to β-actin are indicated below the blot. (**d**) Time course of tumor growth in NSG mice treated with TS or left untreated. Mean values (squares) are plotted. Areas under the curve, a metric of tumor growth that ranged from 112 to 250 in four experimental groups, are also indicated.

shRNA during the 28-day growth period. These results demonstrated that genetic targeting of FOXM1 inhibits myeloma *in vivo*.

Enforced expression of FOXM1 promotes myeloma *in vitro*

To complement the KD studies described above with the opposite experimental approach, we assessed whether enforced transgenic expression of FOXM1 might enhance myeloma growth. To that end, we transfected two independent HMCLs containing moderate amounts of FOXM1 protein, CAG and XG1, with lentivirus that encoded a *FOXM1* cDNA gene under control of the EF1α promoter. Compared with cells transduced with noncoding 'empty' virus that left *FOXM1* levels unchanged (FOXM1^{N}, used as control), cells overexpressing FOXM1 (FOXM1^{OE}) contained elevated amounts of *FOXM1* message (Figure 4a, top) and FOXM1 protein (Figure 4a, bottom). Upregulation of FOXM1 promoted cell growth (Figure 4b), which was abolished by the FOXM1-inhibiting thiazole antibiotic, TS[42] (Supplementary Figure 5a). Increased growth of FOXM1^{OE} cells was attributed to enhanced cell cycle progression (not shown) and survival. The latter was reflected by less pronounced activation of PARP and caspases in FOXM1^{OE} cells compared to FOXM1^{N} cells (Figure 4c). Clonogenic growth in soft agar was moderately heightened (by ~30%) in untreated FOXM1^{OE} vs FOXM1^{N} cells, but more significantly elevated (2–3-fold) in TS-treated FOXM1^{OE} vs FOXM1^{N} cells (Supplementary Figures 5b and c). These results agreed with the FOXM1 KD studies and strengthened the contention that FOXM1 regulates growth and survival of myeloma cells *in vitro*.

OE of FOXM1 promotes myeloma xenografts in NSG mice

We transferred FOXM1^{OE} and FOXM1^{N} CAG cells to NSG mice treated with TS or left untreated (Figure 5a, top). In all cases, FOXM1^{OE} tumors harvested at study endpoint (day 28) were larger than the FOXM1^{N} tumors (Figure 5a, bottom). In untreated mice, the mean weight of FOXM1^{OE} tumors (3.97 g) was significantly higher compared with that of FOXM1^{N} tumors (0.848 g): a ratio of 4.7 (Figure 5b). The OE-to-N ratio (2.03 g/0.432 g, 4.7) was the same in TS-treated mice (Figure 5b), which agreed with the expectation that TS inhibits FOXM1-expressing tumors, but did not support the possibility that FOXM1^{OE} tumors were more sensitive to the drug compared with that of their FOXM1^{N} counterparts. In both TS-treated and -untreated mice, FOXM1^{OE} tumors contained elevated levels of FOXM1 protein relative to FOXM1^{N} controls (Figure 5c). Time-course analyses of tumor size, analogous to those carried out in the KD studies, underlined the myeloma-promoting effect of FOXM1. Using the area under the curve as metric, growth rates of FOXM1^{OE} tumors (198) were elevated by 77% in TS-treated mice compared with FOXM1^{N} tumors (112; Figure 5d). Similarly, in untreated mice, growth rates of FOXM1^{OE} tumors (250) were 83% higher compared with that of FOXM1^{N} tumors (137; Figure 5d). These results added confidence

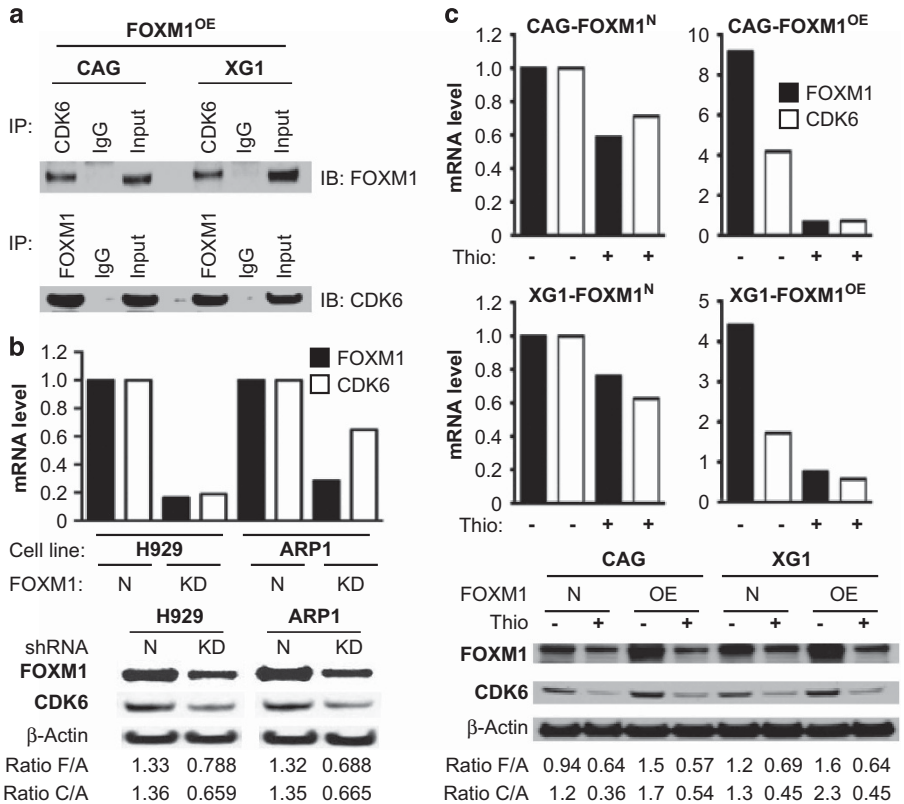

Figure 6. Physical interaction and coexpression of FOXM1 and CDK6 in myeloma cells. (**a**) Co-immunoprecipitation (Co-IP) result indicating physical interaction of FOXM1 and CDK6 in FOXM1-overexpressing (OE) CAG cells (left) and XG1 cells (right). Immunoblots using specific antibodies (Ab's) to FOXM1 (after IP using Ab to CDK6) or CDK6 (after IP using Ab to FOXM1) are shown on top of each other. IgG isotype controls (labeled 'IgG') and samples of whole-cell lysates not subjected to Co-IP (labeled 'Input') were included as controls. (**b**) *FOXM1* message (black bars) and *CDK6* message (white bars) determined by qRT-PCR (top) and corresponding protein levels determined by immunoblotting (bottom) in FOXM1^{KD} and FOXM1^{N} H929 (left) and XG1 (right) myeloma cells. The ratios of target proteins to the housekeeping protein, β-actin, are indicated below the western blots. F/A and C/A denote the ratios including FOXM1 and CDK6, respectively. (**c**) *FOXM1* and *CDK6* mRNA (top) and protein (bottom) levels in FOXM1^{OE} and FOXM1^{N} CAG or XG1 myeloma cells treated with TS (+) or left untreated (−). F/A and C/A ratios are as in panel b.

to the contention that FOXM1 promotes myeloma *in vivo*, yet also indicated that TS may not be as active in mice as it is *in vitro*.

Coordinated expression of FOXM1 and CDK6 in myeloma

To elucidate the mechanism by which FOXM1 promotes myeloma, we followed up on publicly available UCSC ChIP-Seq results and published findings,[43] both indicating that *CDK6* is a transcriptional target of FOXM1 in normal and malignant cells. There is also strong evidence that FOXM1 is a direct phosphorylation target of CDK6 in cancer, suggesting a positive autoregulatory FOXM1-CDK6 feedforward loop that supports the malignant state.[44] Co-IP analysis of FOXM1^{OE} CAG and XG1 cells—which demonstrated that antibody to CDK6 (bait) pulled down FOXM1 (Figure 6a, top), whereas antibody to FOXM1 (bait) pulled down CDK6 (Figure 6a, bottom)—pointed to physical interaction of both proteins in myeloma cells. Codetection of FOXM1 and CDK6 in FOXM1^{OE} CAG cells by means of immunofluorescence microscopy supported this interpretation (not shown). qRT-PCR (Figure 6b, top) and western blotting (Figure 6b, bottom) of FOXM1^{KD} and FOXM1^{N} H929 and ARP1 cells showed that FOXM1 and CDK6 expression may be coregulated in myeloma. Consistent with that, pharmacological inhibition of FOXM1 using TS caused a coordinated drop of *FOXM1* and *CDK6* message in CAG and XG1 cells—more steeply in FOXM1^{OE} than FOXM1^{N} cells (Figure 6c, top). Corresponding changes in FOXM1 protein levels were also seen, but their magnitude was not as high as in case of mRNA (Figure 6c, bottom). In sync with the laboratory findings, *FOXM1* and *CDK6* expression were correlated in the TT2 and TT3 patient cohorts (Supplementary Figure 5b) and predictive of survival (Supplementary Figure 5c). Interestingly, before adopting the UAMS-70 gene signature for stratifying standard- and high-risk myeloma,[2] a 3-gene minisignature had been developed for the same purpose. It relied on *CDK6*; one of its regulators, *CKS1B*, which encodes a member of the highly conserved cyclin kinase subunit 1 family of proteins;[45] and *OPN3* (opsin 3), the role of which in myeloma is obscure (FZ, unpublished result).

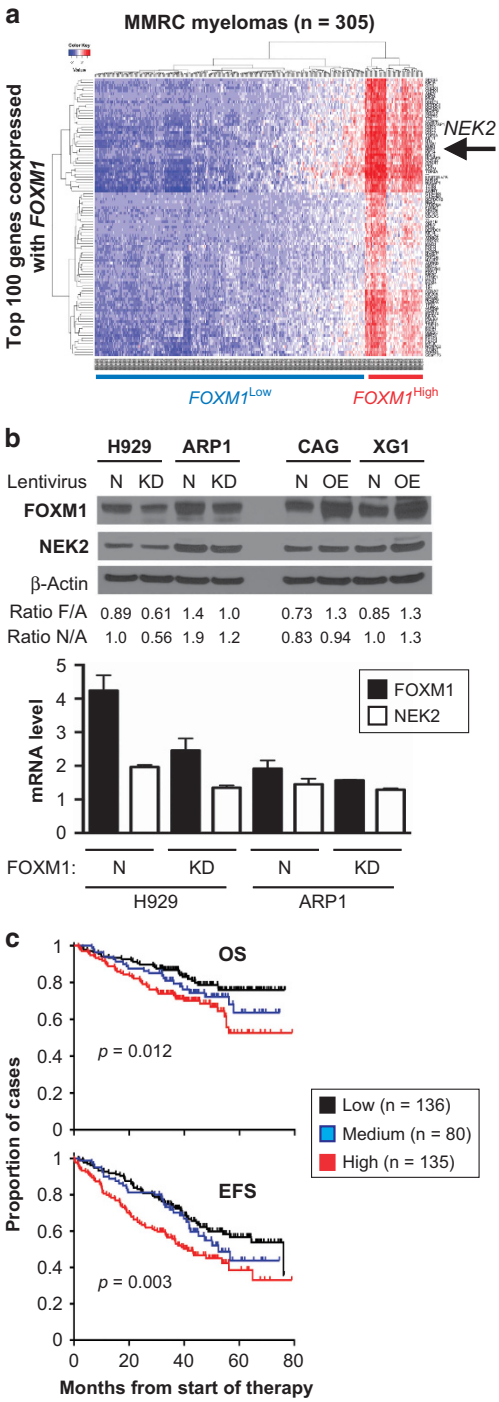

Coexpression of *FOXM1* and *NEK2* in myeloma

To identify additional network genes that may collaborate with *FOXM1* in promoting myeloma, we interrogated the MMRC data set available online for genes tightly coexpressed with *FOXM1* (Figure 7a). Among the top 10 genes ($r^2 = 0.838$) was NIMA-related kinase 2 or *NEK2*. Because NEK2 is not only a well-established transcriptional target of FOXM1 in various cell lineages[46,47] but also a driver of drug resistance in myeloma and other cancers,[48–50] we sought to confirm the coexpression of *NEK2* and *FOXM1* in independent data sets. This was the case in TT2 and TT3 (Supplementary Figure 6a, left) and also in MMRF's CoMMpass^{SM} study (Supplementary Figure 6a, right), in which *FOXM1*^{High} status conferred the same kind of survival disadvantage (Supplementary Figure 6b) seen in the TT2 (Figure 1b) and TT3 (Supplementary Figure 1) cohorts. In the CoMMpass^{SM} data set, *NEK2* was among the top 20 differentially expressed genes ($P = 0.000331$) in a 130-gene list ($P < 0.05$) that distinguished FOXM1^{High} from FOXM1^{Low} tumors (Supplementary Figure 6c). Gene set enrichment

Figure 7. Coordinated expression of FOXM1 and NEK2 in myeloma cells. (**a**) Coexpression of *FOXM1* and *NEK2* in the MMRC data set (305 patients) publicly available at the Broad Institute's Myeloma Genome Portal. The heat map contains the top 100 genes coexpressed with *FOXM1*. Each row and column represents one specific gene and patient, respectively. The position of *NEK2*, which is among the top 10 coregulated genes, is indicated by a labeled arrow that points left. (**b**) Shown at top is an immunoblot analysis of the FOXM1 and NEK2 protein levels in paired FOXM1^{KD}/FOXM1^{N} samples of H929 and ARP1 myeloma cells (left) or paired FOXM1^{OE}/FOXM1^{N} samples of CAG and XG1 myeloma cells (right). The ratios of target to housekeeping protein (β-actin) are indicated below the western blots: F/A for FOXM1 and N/A for NEK2. Presented at the bottom is the result of a qRT-PCR analysis of *FOXM1* and *NEK2* expression in FOXM1^{KD} and FOXM1^{N} H929 (left) and ARP1 (right) cells, demonstrating that genetic downregulation of *FOXM1* leads to a corresponding drop in *NEK2* message. (**c**) Expression levels of *FOXM1* and *NEK2* are associated with survival in TT2 myeloma patients. Cases were stratified as high or low expressers when both *FOXM1* and *NEK2* message were above (indicated in red) or below (black) the medium level in the TT2 data set. All remaining cases (i.e., FOXM1^{High}/NEK2^{Low} or FOXM1^{Low}/NEK2^{High}) were designated as medium expressers (blue). EFS and OS in all three groups was plotted and statistically compared using log-rank analysis.

analysis using this gene list as the input revealed a FOXM1-dependent network of transcription factors, DNA replication and cell division pathways in myeloma (Supplementary Figure 6d). These *in silico* findings prompted us to determine whether *FOXM1* and *NEK2* might be coexpressed in the four HMCLs used throughout this study. Western blotting showed that FOXM1 and NEK2 proteins shifted coordinately in accordance with FOXM1 status in four of four cell lines (Figure 7b, top). At the message level, results were less consistent; that is, although *NEK2* mRNA dropped upon KD of *FOXM1* in H929 and ARP1 cells (Figure 7b, bottom), *NEK2* did not rise upon OE of *FOXM1* in CAG and XG1 cells (results not shown). Despite the latter finding, *FOXM1* and *NEK2* expression status was statistically linked with survival in the TT2 cohort (Figure 7c). These results provided evidence that *FOXM1* and *NEK2* are coregulated in myeloma.

DISCUSSION

The main finding of this study is clinical and experimental evidence for the involvement of FOXM1 in a relatively small (~15%) but aggressive subset of myeloma (chiefly subgroups MF and PR). *FOXM1* expands the list of candidate genes uncovered by us[35,38,48,51] and others,[52,53] which seem to render myeloma a high-risk disease by regulating pathways of tumor progression and stemness, acquisition of drug resistance and, ultimately, refractory relapse. A distinctive feature of *FOXM1*, compared with all other candidate genes identified thus far, is its discovery in a comprehensive gene expression analysis of mature B-cell lymphoma counterparts in humans and mice.[14] Cross-species analyses of this sort, which afford a unique and powerful approach to identifying genetic networks of neoplastic growth conserved over millions of years of evolution, have been successfully used in research on solid cancers but largely neglected in myeloma.[14] The results on *FOXM1* reported here demonstrate the utility of this approach for myeloma and suggest that comparative oncogenomics of myeloma-like tumors in genetically engineered mouse models may not only further our understanding of the natural history of myeloma but also reveal new targets for treatment and prevention. The ongoing development of new genetically engineered mouse models[54–56] and continuous refinement of established ones[57–59] are generating great promise along this line.

The results reported here may be summarized in a working model of FOXM1's function in myeloma (Figure 8a), which considers (1) the gene's coregulation with CDK6 and NEK2, (2) the output of a network analysis that relied on the GeneMANIA online tool to predict genetic interactions of FOXM1 in myeloma cells (Figure 8b) and (3) the ability of a novel 3-gene minisignature, comprised of *FOXM1*, *CDK6* and *NEK2*, to prognosticate survival of patients with myeloma (Figure 8c). Although the underlying molecular genetics of the interaction depicted in Figure 8a needs to be elucidated in greater depth, the scheme may provide a useful blueprint for designing combination treatments for FOXM1^{High} myelomas. This may take advantage of small-molecule inhibitors of (a) FOXM1, such as FDI-6, which binds directly to the transcription factor and displaces it from genomic targets in cancer cells,[27] (b) CDK6, such as palbociclib, which is not

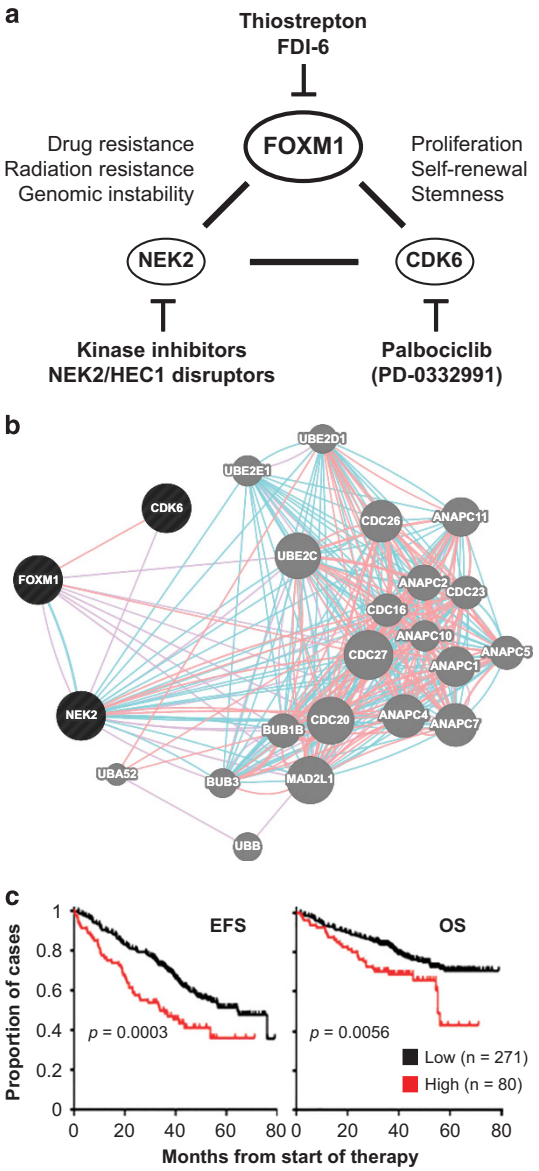

Figure 8. FOXM1 may interact with CDK6 and NEK2 to shorten survival of patients with high-risk myeloma. (**a**) Working model on the interaction of FOXM1, CDK6 and NEK2 in myeloma. Although FOXM1 is most firmly established as a proliferation-associated gene, new findings indicating that FOXM1 governs self-renewal and tumorigenicity of cancer stem cell-like cells in glioblastoma,[25] and that the FOXM1 target, CDK6, serves as a key regulator of leukemia stem cell activation,[64] raise the possibility that the interaction of FOXM1 and CDK6 in myeloma is also important for stemness. Additionally, FOXM1 may collaborate with NEK2 to drive resistance of myeloma cells to cancer therapy, given that NEK2 has been implicated in acquired drug resistance of many cancers[48–50] and specifically shown to activate certain ABC drug transporters in myeloma.[48] Specific inhibitors of all three genes have been developed. Palbocicblib has already demonstrated activity in clinical trials on myeloma. (**b**) Genetic interaction network of FOXM1, CDK6 and NEK2 (indicated in black to the left) generated with the help of the GeneMANIA online tool. Blue and pink lines denote pathways and physical interactions, respectively. Network genes are indicated by gray circles to the right that are labeled. The network's apparent enrichment for ubiquination genes (not shown) points to the proteasome, suggesting in turn that the FOXM1-CDK6-NEK2 network core is involved in the response of myeloma cells to proteasome inhibition, a widely used treatment for myeloma. (**c**) Kaplan–Meier plots of EFS (left) and OS (right) of patients with myeloma from the TT2 cohort stratified according to high levels (red) or low levels (black) of *FOXM1*, *CDK6* and *NEK2* message upon microarray analysis. Myelomas containing higher than median amounts of mRNA of *all three* genes were designated as high ($n = 80$), whereas myelomas that did not meet this criterion were designated as low ($n = 271$). The differences in survival were significant using log-rank analysis ($P < 0.05$).

highly specific (it also targets CDK4) but has already demonstrated therapeutic activity (in conjunction with bortezomib and dexamethasone) in a phase 1/2 clinical trial of relapsed/refractory MM[60] and (c) NEK2, such as aminopyridine scaffold compounds, which inhibit NEK2's kinase activity,[61] or unrelated inhibitors, which trigger NEK2 degradation indirectly, using a mechanism that involves the disruption of NEK2 binding to kinetochore complex component, NDC80, better known as highly expressed in cancer 1 or HEC1.[62] Despite broad cancer-suppressing activities,[63] the cyclic oligopeptide antibiotic, TS, which has been used here as a FOXM1-inhibiting compound, is an unlikely candidate for further therapeutic development because its extensive use in veterinary medicine revealed severe toxicity issues.

In conclusion, *FOXM1* appears to be a bone fide high-risk myeloma gene that interacts with *CDK6* and *NEK2* to facilitate myeloma xenografts in mice and promote the growth, clonogenic self-renewal and survival of myeloma cells *in vitro*. Clinical studies are warranted to further validate FOXM1 as a potential therapeutic target in FOXM1^{High} high-risk myeloma.

CONFLICT OF INTEREST

The authors declare no conflict of interest.

ACKNOWLEDGEMENTS

The expert technical assistance by Dr Xuefang Jing and the provision of NSG mice by Dr Weizhou Zhang (both Department of Pathology, University of Iowa) are gratefully acknowledged. Research funding in Germany (Heidelberg) was provided by the Dietmar Hopp Stiftung (Walldorf), the Systems Medicine program of the German Ministry of Education and Science (CLIOMMICS 01ZX1309), and the Deutsche Forschungsgemeinschaft (Sonderforschungsbereich/Transregio TRR79). This work was supported in part by NIH Training Grant T32-HL07734 and National Natural Science Foundation of China (NNSFC) Grant 81250110552 (both to VT); by NCI R01CA152105, Leukemia & Lymphoma Society Translational Research Program Awards 6246-11 and 6094-12, NNSFC Award 81228016, Multiple Myeloma Research Foundation Senior Research Program Award 2015 and International Myeloma Foundation Senior Research Program Award 2015 (all to FZ); by institutional start-up funds from the Department of Internal Medicine, CCOM, UI (to FZ and GT); by NCI Core Grant P30CA086862 in support of The University of Iowa Holden Comprehensive Cancer Center; and by NCI R01CA151354 (to SJ).

REFERENCES

1 Zhan F, Huang Y, Colla S, Stewart JP, Hanamura I, Gupta S *et al.* The molecular classification of multiple myeloma. *Blood* 2006; **108**: 2020–2028.
2 Shaughnessy Jr JD, Zhan F, Burington BE, Huang Y, Colla S, Hanamura I *et al.* A validated gene expression model of high-risk multiple myeloma is defined by deregulated expression of genes mapping to chromosome 1. *Blood* 2007; **109**: 2276–2284.
3 Kuiper R, Broyl A, de Knegt Y, van Vliet MH, van Beers EH, van der Holt B *et al.* A gene expression signature for high-risk multiple myeloma. *Leukemia* 2012; **26**: 2406–2413.
4 Wu P, Walker BA, Broyl A, Kaiser M, Johnson DC, Kuiper R *et al.* A gene expression based predictor for high risk myeloma treated with intensive therapy and autologous stem cell rescue. *Leuk Lymphoma* 2015; **56**: 594–601.
5 Rajkumar SV. Multiple myeloma: 2012 update on diagnosis, risk-stratification, and management. *Am J Hematol* 2012; **87**: 78–88.
6 Koo CY, Muir KW, Lam EW. FOXM1: from cancer initiation to progression and treatment. *Biochim Biophys Acta* 2012; **1819**: 28–37.
7 Gong A, Huang S. FoxM1 and Wnt/beta-catenin signaling in glioma stem cells. *Cancer Res* 2012; **72**: 5658–5662.
8 Matsui W, Wang Q, Barber JP, Brennan S, Smith BD, Borrello I *et al.* Clonogenic multiple myeloma progenitors, stem cell properties, and drug resistance. *Cancer Res* 2008; **68**: 190–197.
9 Hajek R, Okubote SA, Svachova H. Myeloma stem cell concepts, heterogeneity and plasticity of multiple myeloma. *Br J Haematol* 2013; **163**: 551–564.
10 Wonsey DR, Follettie MT. Loss of the forkhead transcription factor FoxM1 causes centrosome amplification and mitotic catastrophe. *Cancer Res* 2005; **65**: 5181–5189.
11 Laoukili J, Stahl M, Medema RH. FoxM1: at the crossroads of ageing and cancer. *Biochim Biophys Acta* 2007; **1775**: 92–102.
12 Neri P, Bahlis NJ. Genomic instability in multiple myeloma: mechanisms and therapeutic implications. *Expert Opin Biol Ther* 2013; **13** (Suppl 1): S69–S82.
13 Uddin S, Hussain AR, Ahmed M, Siddiqui K, Al-Dayel F, Bavi P *et al.* Overexpression of FoxM1 offers a promising therapeutic target in diffuse large B-cell lymphoma. *Haematologica* 2012; **97**: 1092–1100.
14 Tompkins VS, Han SS, Olivier A, Syrbu S, Bair T, Button A *et al.* Identification of candidate B-lymphoma genes by cross-species gene expression profiling. *PLoS One* 2013; **8**: e76889.
15 Kong X, Li L, Li Z, Le X, Huang C, Jia Z *et al.* Dysregulated expression of FOXM1 isoforms drives progression of pancreatic cancer. *Cancer Res* 2013; **73**: 3987–3996.
16 Cai Y, Balli D, Ustiyan V, Fulford L, Hiller A, Misetic V *et al.* Foxm1 expression in prostate epithelial cells is essential for prostate carcinogenesis. *J Biol Chem* 2013; **288**: 22527–22541.
17 Wang Z, Zheng Y, Park HJ, Li J, Carr JR, Chen YJ *et al.* Targeting FoxM1 effectively retards p53-null lymphoma and sarcoma. *Mol Cancer Ther* 2013; **12**: 759–767.
18 Motiwala T, Kutay H, Zanesi N, Frissora FW, Mo X, Muthusamy N *et al.* PTPROt-mediated regulation of p53/Foxm1 suppresses leukemic phenotype in a CLL mouse model. *Leukemia* 2015; **29**: 1350–1359.
19 Kopanja D, Pandey A, Kiefer M, Wang Z, Chandan N, Carr JR *et al.* Essential roles of FoxM1 in Ras-induced liver cancer progression and in cancer cells with stem cell features. *J Hepatol* 2015; **63**: 429–436.
20 Zona S, Bella L, Burton MJ, Nestal de Moraes G, Lam EW. FOXM1: an emerging master regulator of DNA damage response and genotoxic agent resistance. *Biochim Biophys Acta* 2014; **1839**: 1316–1322.
21 Teh MT, Gemenetzidis E, Patel D, Tariq R, Nadir A, Bahta AW *et al.* FOXM1 induces a global methylation signature that mimics the cancer epigenome in head and neck squamous cell carcinoma. *PLoS One* 2012; **7**: e34329.
22 Eckers JC, Kalen AL, Sarsour EH, Tompkins VS, Janz S, Son JM *et al.* Forkhead box M1 regulates quiescence-associated radioresistance of human head and neck squamous carcinoma cells. *Radiat Res* 2014; **182**: 420–429.
23 Karunarathna U, Kongsema M, Zona S, Gong C, Cabrera E, Gomes AR *et al.* OTUB1 inhibits the ubiquitination and degradation of FOXM1 in breast cancer and epirubicin resistance. *Oncogene* 2016; **35**: 1433–1444.
24 Hou Y, Li W, Sheng Y, Li L, Huang Y, Zhang Z *et al.* The transcription factor Foxm1 is essential for the quiescence and maintenance of hematopoietic stem cells. *Nat Immunol* 2015; **16**: 810–818.
25 Gong AH, Wei P, Zhang S, Yao J, Yuan Y, Zhou AD *et al.* FoxM1 drives a feed-forward STAT3-activation signaling loop that promotes the self-renewal and tumorigenicity of glioblastoma stem-like cells. *Cancer Res* 2015; **75**: 2337–2348.
26 Chiu WT, Huang YF, Tsai HY, Chen CC, Chang CH, Huang SC *et al.* FOXM1 confers to epithelial-mesenchymal transition, stemness and chemoresistance in epithelial ovarian carcinoma cells. *Oncotarget* 2015; **6**: 2349–2365.
27 Gormally MV, Dexheimer TS, Marsico G, Sanders DA, Lowe C, Matak-Vinkovic D *et al.* Suppression of the FOXM1 transcriptional programme via novel small molecule inhibition. *Nat Commun* 2014; **5**: 5165.
28 Halasi M, Gartel AL. Targeting FOXM1 in cancer. *Biochem Pharmacol* 2013; **85**: 644–652.
29 Gazdar AF, Oie HK, Kirsch IR, Hollis GF. Establishment and characterization of a human plasma cell myeloma culture having a rearranged cellular myc proto-oncogene. *Blood* 1986; **67**: 1542–1549.
30 Zhang XG, Gaillard JP, Robillard N, Lu ZY, Gu ZJ, Jourdan M *et al.* Reproducible obtaining of human myeloma cell lines as a model for tumor stem cell study in human multiple myeloma. *Blood* 1994; **83**: 3654–3663.
31 Feinman R, Koury J, Thames M, Barlogie B, Epstein J, Siegel DS. Role of NF-kappaB in the rescue of multiple myeloma cells from glucocorticoid-induced apoptosis by bcl-2. *Blood* 1999; **93**: 3044–3052.
32 Baughn LB, Di Liberto M, Wu K, Toogood PL, Louie T, Gottschalk R *et al.* A novel orally active small molecule potently induces G1 arrest in primary myeloma cells and prevents tumor growth by specific inhibition of cyclin-dependent kinase 4/6. *Cancer Res* 2006; **66**: 7661–7667.
33 Lombardi L, Poretti G, Mattioli M, Fabris S, Agnelli L, Bicciato S *et al.* Molecular characterization of human multiple myeloma cell lines by integrative genomics: insights into the biology of the disease. *Genes Chromosomes Cancer* 2007; **46**: 226–238.
34 Yellapantula V, Divya T, Dinu V, Scotch M. Informatics approaches for integrative analysis of disparate high-throughput genomic datasets in cander. Arizona State University (ASU) Electronic Dissertations and Theses Digital Repository, 2014.
35 Yang Y, Shi J, Tolomelli G, Xu H, Xia J, Wang H *et al.* RARalpha2 expression confers myeloma stem cell features. *Blood* 2013; **122**: 1437–1447.
36 Hurt EM, Wiestner A, Rosenwald A, Shaffer AL, Campo E, Grogan T *et al.* Overexpression of c-maf is a frequent oncogenic event in multiple myeloma that

promotes proliferation and pathological interactions with bone marrow stroma. *Cancer Cell* 2004; **5**: 191–199.
37 Romagnoli M, Trichet V, David C, Clement M, Moreau P, Bataille R *et al.* Significant impact of survivin on myeloma cell growth. *Leukemia* 2007; **21**: 1070–1078.
38 Yang Y, Shi J, Gu Z, Salama ME, Das S, Wendlandt E *et al.* Bruton tyrosine kinase is a therapeutic target in stem-like cells from multiple myeloma. *Cancer Res* 2015; **75**: 594–604.
39 Weiss BM, Abadie J, Verma P, Howard RS, Kuehl WM. A monoclonal gammopathy precedes multiple myeloma in most patients. *Blood* 2009; **113**: 5418–5422.
40 van Rhee F, Szymonifka J, Anaissie E, Nair B, Waheed S, Alsayed Y *et al.* Total Therapy 3 for multiple myeloma: prognostic implications of cumulative dosing and premature discontinuation of VTD maintenance components, bortezomib, thalidomide, and dexamethasone, relevant to all phases of therapy. *Blood* 2010; **116**: 1220–1227.
41 Seckinger A, Meissner T, Moreaux J, Depeweg D, Hillengass J, Hose K *et al.* Clinical and prognostic role of annexin A2 in multiple myeloma. *Blood* 2012; **120**: 1087–1094.
42 Hegde NS, Sanders DA, Rodriguez R, Balasubramanian S. The transcription factor FOXM1 is a cellular target of the natural product thiostrepton. *Nat Chem* 2011; **3**: 725–731.
43 Sanders DA, Gormally MV, Marsico G, Beraldi D, Tannahill D, Balasubramanian S. FOXM1 binds directly to non-consensus sequences in the human genome. *Genome Biol* 2015; **16**: 130.
44 Anders L, Ke N, Hydbring P, Choi YJ, Widlund HR, Chick JM *et al.* A systematic screen for CDK4/6 substrates links FOXM1 phosphorylation to senescence suppression in cancer cells. *Cancer Cell* 2011; **20**: 620–634.
45 Chang H, Jiang N, Jiang H, Saha MN, Qi C, Xu W *et al.* CKS1B nuclear expression is inversely correlated with p27Kip1 expression and is predictive of an adverse survival in patients with multiple myeloma. *Haematologica* 2010; **95**: 1542–1547.
46 Nischalke HD, Schmitz V, Luda C, Aldenhoff K, Berger C, Feldmann G *et al.* Detection of IGF2BP3, HOXB7, and NEK2 mRNA expression in brush cytology specimens as a new diagnostic tool in patients with biliary strictures. *PLoS One* 2012; **7**: e42141.
47 Calvisi DF, Pinna F, Ladu S, Pellegrino R, Simile MM, Frau M *et al.* Forkhead box M1B is a determinant of rat susceptibility to hepatocarcinogenesis and sustains ERK activity in human HCC. *Gut* 2009; **58**: 679–687.
48 Zhou W, Yang Y, Xia J, Wang H, Salama ME, Xiong W *et al.* NEK2 induces drug resistance mainly through activation of efflux drug pumps and is associated with poor prognosis in myeloma and other cancers. *Cancer Cell* 2013; **23**: 48–62.
49 Liu X, Gao Y, Lu Y, Zhang J, Li L, Yin F. Upregulation of NEK2 is associated with drug resistance in ovarian cancer. *Oncol Rep* 2014; **31**: 745–754.
50 Marina M, Saavedra HI. Nek2 and Plk4: prognostic markers, drivers of breast tumorigenesis and drug resistance. *Front Biosci (Landmark Ed)* 2014; **19**: 352–365.
51 Shi L, Wang S, Zangari M, Xu H, Cao TM, Xu C *et al.* Over-expression of CKS1B activates both MEK/ERK and JAK/STAT3 signaling pathways and promotes myeloma cell drug-resistance. *Oncotarget* 2010; **1**: 22–33.
52 Tanno T, Lim Y, Wang Q, Chesi M, Bergsagel PL, Matthews G *et al.* Growth Differentiating Factor 15 enhances the tumor initiating and self-renewal potential of multiple myeloma cells. *Blood* 2013; **123**: 725–733.
53 Ziv E, Dean E, Hu D, Martino A, Serie D, Curtin K *et al.* Genome-wide association study identifies variants at 16p13 associated with survival in multiple myeloma patients. *Nat Commun* 2015; **6**: 7539.
54 Hu Y, Zheng M, Gali R, Tian Z, Topal Gorgun G, Munshi NC *et al.* A novel rapid-onset high-penetrance plasmacytoma mouse model driven by deregulation of cMYC cooperating with KRAS12V in BALB/c mice. *Blood Cancer J* 2013; **3**: e156.
55 Dechow T, Steidle S, Gotze KS, Rudelius M, Behnke K, Pechloff K *et al.* GP130 activation induces myeloma and collaborates with MYC. *J Clin Invest* 2014; **124**: 5263–5274.
56 Tompkins VS, Rosean TR, Holman CJ, DeHoedt C, Olivier AK, Duncan KM *et al.* Adoptive B-cell transfer mouse model of human myeloma. *Leukemia* 2016; **30**: 962–966.
57 Chesi M, Matthews GM, Garbitt VM, Palmer SE, Shortt J, Lefebure M *et al.* Drug response in a genetically engineered mouse model of multiple myeloma is predictive of clinical efficacy. *Blood* 2012; **120**: 376–385.
58 Lee EC, Fitzgerald M, Bannerman B, Donelan J, Bano K, Terkelsen J *et al.* Antitumor activity of the investigational proteasome inhibitor MLN9708 in mouse models of B-cell and plasma cell malignancies. *Clin Cancer Res* 2011; **17**: 7313–7323.
59 Duncan K, Rosean TR, Tompkins VS, Olivier A, Sompallae R, Zhan F *et al.* (18)F-FDG-PET/CT imaging in an IL-6- and MYC-driven mouse model of human multiple myeloma affords objective evaluation of plasma cell tumor progression and therapeutic response to the proteasome inhibitor ixazomib. *Blood Cancer J* 2013; **3**: e165.
60 Niesvizky R, Badros AZ, Costa LJ, Ely SA, Singhal SB, Stadtmauer EA *et al.* Phase 1/2 study of cyclin-dependent kinase (CDK)4/6 inhibitor palbociclib (PD-0332991) with bortezomib and dexamethasone in relapsed/refractory multiple myeloma. *Leuk Lymphoma* 2015; **56**: 3320–3328.
61 Innocenti P, Woodward H, O'Fee L, Hoelder S. Expanding the scope of fused pyrimidines as kinase inhibitor scaffolds: synthesis and modification of pyrido[3,4-d]pyrimidines. *Org Biomol Chem* 2015; **13**: 893–904.
62 Hu CM, Zhu J, Guo XE, Chen W, Qiu XL, Ngo B *et al.* Novel small molecules disrupting Hec1/Nek2 interaction ablate tumor progression by triggering Nek2 degradation through a death-trap mechanism. *Oncogene* 2015; **34**: 1220–1230.
63 Bhat UG, Halasi M, Gartel AL. FoxM1 is a general target for proteasome inhibitors. *PLoS One* 2009; **4**: e6593.
64 Scheicher R, Hoelbl-Kovacic A, Bellutti F, Tigan AS, Prchal-Murphy M, Heller G *et al.* CDK6 as a key regulator of hematopoietic and leukemic stem cell activation. *Blood* 2015; **125**: 90–101.

Supplementary Information accompanies this paper on the Leukemia website (http://www.nature.com/leu)